Modular synchronization in complex networks

E. Oh,[1] K. Rho,[1] H. Hong,[2] and B. Kahng[1]

[1]*School of Physics and Center for Theoretical Physics, Seoul National University, Seoul 151-747, Korea*
[2]*Department of Physics, Chonbuk National University, Jeonju, 561-756, Korea*

We study the synchronization transition (ST) of a modified Kuramoto model on two different types of modular complex networks. It is found that the ST depends on the type of intermodular connections. For the network with decentralized (centralized) intermodular connections, the ST occurs at finite coupling constant (behaves abnormally). Such distinct features are found in the yeast protein interaction network and the Internet, respectively. Moreover, by applying the finite-size scaling analysis to an artificial network with decentralized intermodular connections, we obtain the exponent associated with the order parameter of the ST to be $\beta \approx 1$ different from $\beta_{MF} \approx 1/2$ obtained from the scale-free network with the same degree distribution but the absence of modular structure, corresponding to the mean field value.

Recently, there have been considerable efforts to understand complex systems in terms of graph, consisting of vertices and edges [1]. An interesting feature emerging in such complex networks is a power-law degree distribution, $P_d(k) \sim k^{-\gamma}$, where degree k is the number of edges incident upon a given vertex. Such networks are called scale-free (SF) networks [2]. Many SF networks in real world such as the yeast protein interaction networks (PINs), the Internet, and social networks contain modular structures within them [3–6]. While recent studies have focused on the identification or classification of such modules [7], little attention has been paid to how such modules are interconnected to each other [8]. In this paper, we study the synchronization transition (ST) emerging from such modular SF networks. It is found that the feature of the ST depends on the types of the intermodular connections, different from that occurring on the SF network without modules.

Synchronization phenomena can be found in diverse fields [9,10], which have been studied through coupled oscillator models [11]. Here, we study the dynamics of synchronization on SF networks through a modified Kuramoto model [12],

$$\frac{d\phi_i}{dt} = \omega_i - \frac{K}{k_i} \sum_{j \in nn \text{ of } i} \sin(\phi_i - \phi_j), \qquad (1)$$

where ϕ_i and ω_i are the phase and the intrinsic frequency of vertex i, respectively. ω_i is chosen from the Gaussian distribution with unit variance. The summation runs over j, the nearest neighbors (nn) of vertex i. Note that in contrast to other works [11,12], the coupling strength is used as K/k_i, where k_i is the degree of vertex i. Due to the factor $1/k_i$, the dephasing effect at the vertex with large degree is reduced [13], and the ST occurs at finite K_c in SF networks even for $2 < \gamma < 3$ [14]. Note that when the factor $1/k_i$ is absent, $K_c = 0$ for SF networks with $2 < \gamma < 3$ [14,15]. The order parameter $\mathcal{M}$ is defined as

$$\mathcal{M} \equiv \lim_{t \to \infty} \left\langle \left| \frac{1}{N} \sum_{j=1}^{N} e^{i\phi_j} \right| \right\rangle,$$

where $\langle \cdots \rangle$ is the ensemble average over different configurations and N is the total number of vertices. $\mathcal{M}$ is 0 (1) in the fully incoherent (coherent) phase.

To study how the profile of intermodular connections affects the ST pattern, we first investigate the intermodular connections of two real world networks, the yeast PIN and the Internet at autonomous system level. Although the two networks are not oscillator networks, we use them because they are prototypical examples of modular networks and contain different types of intermodular connections. While a neuronal network is a good example of oscillator networks, its structure has been still veiled. As shown in Fig. 1, the modules of the PIN are interwoven diversely, while those of the Internet are connected mainly through only a single module, corresponding to the North America continent. The synchronization transition patterns occurring on those two networks appear distinct in three aspects. First, as the coupling constant K increases, the order parameter increases very drastically for the former, while it does gradually for the latter (Fig. 2). Quantitatively, the order parameter increases from $\mathcal{M} = 0.2$ to 0.8 by the increment $\delta K = 1.3$ and $\delta K = 2.9$ for the PIN and Internet, respectively. Second, the susceptibility χ, defined as $\chi = \sqrt{\langle (r - \langle r \rangle)^2 \rangle}$ with $r = \lim_{t \to \infty} |(1/N) \sum_{j=1}^{N} e^{i\phi_j}|$, exhibits a peak at the transition point K_c, which is narrow (broad) for the former (latter) (see the inset of Fig. 2). To quantify it, we measure the interquartile range [16], which corresponds to the standard deviation often used for the asymmetric distribution case, to be 1.3 and 3.0 for the PIN and Internet, respectively. Each number means the interval of K where 50% of the data around the peak position belong. Third, when $K \gg K_c$, for the former, most modules are synchronized with almost the same phase, while for the latter, individual modules are synchronized independently, leading the overall system to be weakly synchronized. We also confirm such different types of the synchronization patterns through two artificial networks.
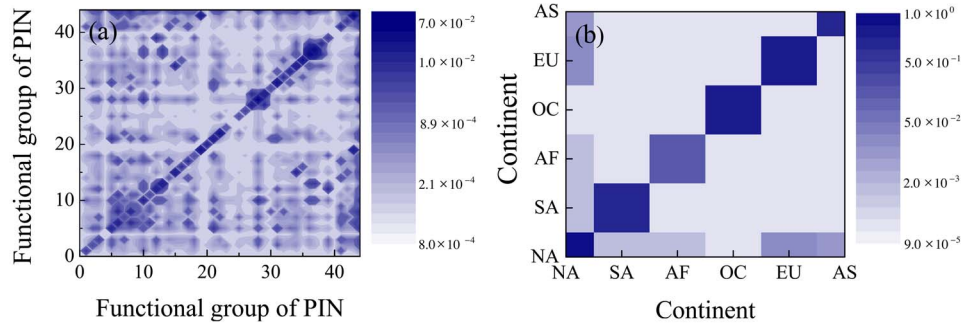
FIG. 1. (Color online). Profile of intermodular connections for the PIN (a) and the Internet (b). The concentration $c_{i,j} = \ell_{i,j}\ell_{j,i}/L_iL_j$, where $\ell_{i,j}$ is the number of edges emanating from module i to module j and the $L_i = \Sigma_j \ell_{i,j}$. NA, SA, AF, OC, EU, and AS stand for North America, South America, Africa, Oceania, Europe, and Asia, respectively.

The two artificial networks are defined as follows: One is a modification of the community model (CM), proposed by Girvin and Newman [7]. There, n_c modules are present from the beginning, which is fixed under evolution, while the total numbers of vertices and edges grow with time. Initially, each module contains m vertices and they are fully connected. At each time step, a new vertex is added to the system and chooses a module at random. The newly added vertex attaches m_0 edges to existing vertices selected with the probability proportional to its degree [2], belonging to the chosen module. This process is repeated until the step when each module contains n_0 vertices on average. Then n_c sets of distinct SF networks are generated. After those steps, we add m_e edges, connecting vertices belonging to different modules, which are selected randomly. The parameters, n_c, n_0, m_0, and m_e are adjustable. To compare the resulting network with the yeast PIN, we take $n_c = 5$ and $n_0 = 625$, $m_0 = 3$ and $m_e = 934$, making the mean degree be 6.58, comparable to that of the PIN, 6.55. While the CM may be too artificial or have too many parameters, it simply reflects the presence of modules and their diverse connections. The second one is the hierarchy model introduced by Ravasz and Barabási [17]. The model contains five modules at the highest level, each of which contains five submodules within it in a hierarchical manner. The intermodular interactions in the hierarchy model are made only through one particular module among the five modules at the same hierarchical level. The mean degree of the hierarchy model is $\langle k \rangle = 7.8$.

The distinct ST patterns can be observed more obviously in the size-dependent behaviors of $\mathcal{M}$ in the CM and the hierarchy model. The system size N is controlled by changing the number of vertices in each module n_0 in the CM and the number of hierarchical levels in the hierarchy model. As shown in Fig. 3, for the CM, the ST occurs at $K_c \simeq 2.1$, which is the crossing point of $\mathcal{M}$ for different sizes. We find numerically that the order parameter scales as $\mathcal{M} \sim N^{-\beta/\mu}F(\Delta N^{1/\mu})$, where $\Delta = K - K_c$, $\beta/\mu \simeq 0.25$, and $1/\mu \simeq 0.25$. Thus $\beta \approx 1$ for the CM network. To check if it is related to the existence of the modular structure, we destroy the modular structure in the CM model by rewiring edges. Two different edges are randomly selected and their one-end vertices are exchanged unless this swap procedure makes the network disconnected. The swapping process is applied as many as two times of the total number of edges. Then the resulting network loses modules but the degree distribution remains the same. Applying the finite-size scaling analysis to the swapped CM network, we obtain the mean field value $\beta_{MF} \approx 1/2$. Thus the nature of the ST is changed by the absence of modular structure. On the other hand, for the hierarchy model, we cannot find any crossing point in $\mathcal{M}$ for different sizes. For small K, the data are well fit to the scaling form of $\mathcal{M} \sim N^{-\beta/\mu}F(KN^{1/\mu})$ with $\beta/\mu \approx 0.5$ and $1/\mu \simeq 0.17$ [Fig. 3(b)].

To understand the emergence of the different ST patterns from a microscopic respect, we identify modules of each network and examine the synchronization within each mod-
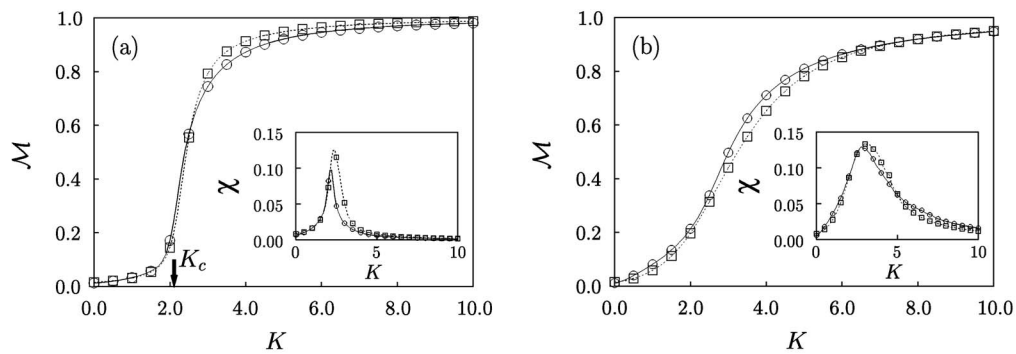

FIG. 2. Plot of the order parameter $\mathcal{M}$ as a function of the coupling constant K for two different types of complex networks, the yeast PIN ($\bigcirc$) and the CM ($\square$) in (a) and the Internet ($\bigcirc$) and the hierarchy model ($\square$) in (b). Insets: plot of the susceptibility as a function of K for each case.
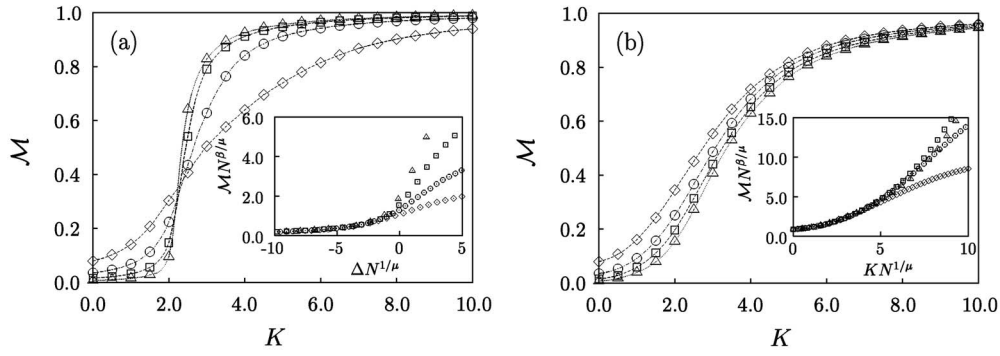
FIG. 3. Size dependence of $\mathcal{M}$ in the CM (a) and the hierarchy model (b). The data are obtained for different system sizes 125 ($\diamond$), 625 ($\bigcirc$), 3125 ($\square$), and 15 625 ($\triangle$) with 1000 configurations for each. Inset: plot of the order parameter in the scaling form.

ule. For the yeast PIN, 43 modules are identified according to their functional categories and for the Internet, six modules are done according to the continents in the world. Modules for the artificial networks can be naturally identified. In Fig. 4, we plot the phase distributions at $K=7.0$ for the four networks. Each curve represents the normalized phase distribution of each module. For the PIN, the phase distributions of each module overlap each other except the three modules called by cell adhesion, mitochondrial transcription, and septation. They have few connections with other modules. Thus the phase distributions of them do not assemble. For the CM, most of the phase distributions overlap each other, implying that the networks are globally synchronized. For the Internet and the hierarchy model, however, the phase distribution functions of each module do not overlap, indicating that each module is synchronized independently. The network is modularly synchronized. Thus the global synchronization for the Internet and the hierarchy model appears weaker than that for the PIN and the CM for the given K.

To see the interplay between the two ST patterns, we deform the network structure of the hierarchy model by swapping edges as used in the CM network. The ratio p between the number of swapping edges and the total number of edges is a control parameter. With increasing p, the intermodular connections are decentralized. As can be seen in Fig. 5, the

ST pattern becomes sharper as the ratio p increases, and in particular it changes drastically up to $p \approx 0.1$, beyond which they look very similar and overlap with the ST data for the PIN or the CM.

It was recently shown that the synchronizability in complex networks is related to the maximum value of load ℓ_{max} [18,19]. Load is the effective amount of data packets passing through a given vertex when every pair of vertices sends and receives a unit data packet along the shortest pathways between them [20]. To examine how ℓ_{max} is related to the synchronization pattern, we investigate ℓ_{max} as a function of the swapping ratio p. As shown in the inset of Fig. 5, ℓ_{max} decreases rapidly in the range of $0 < p < 0.1$, however, it decreases very slowly or is almost constant for $p > 0.1$. This suggests that across $p \approx 0.1$, the synchronizability becomes enhanced drastically, in accordance with the behavior of the $\mathcal{M}$.

It would be interesting to see such a crossover through the Barabási and Albert (BA) model. We control the number of edges m_{BA} emanating from a newly added node in the BA model. When $m_{BA}=1$, $\mathcal{M}$ is almost flat with changing K. For larger m_{BA}, $\mathcal{M}$ changes more sharply with increasing K as shown in Fig. 6. ℓ_{max} decreases drastically up to $m_{BA} \approx 1.1$ and gradually decrease beyond that as shown in the inset of Fig. 6, reflecting that the synchronizability enhances drastically at $m_{BA} \approx 1.1$. This fact is related to the topological feature as follows. When $m_{BA}=1$, the network is a tree. As m_{BA}
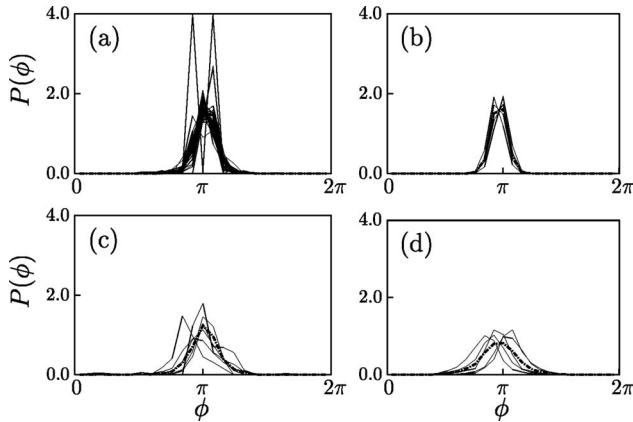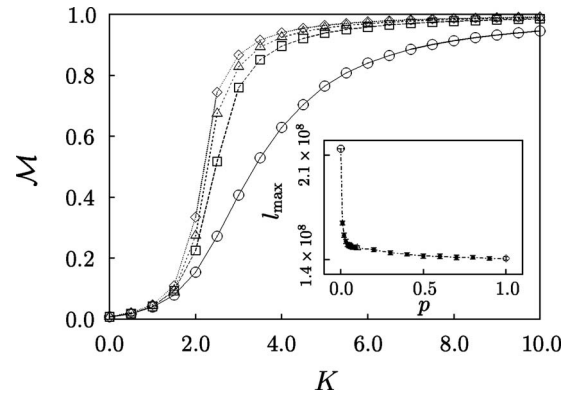

FIG. 4. The normalized phase distribution of each module (solid line) at the coupling constant $K=7.0$ for the PIN (a), the CM (b), the Internet (c), and the hierarchy model (d). The dashed line represents the normalized phase distribution of the overall system.

FIG. 5. The interplay of the ST pattern in the hierarchy model as a function of p, the swapping ratio, for $p=0$ ($\bigcirc$), $p=0.1$ ($\square$), $p=0.5$ ($\triangle$), and $p=1.0$ ($\diamond$). Inset: plot of ℓ_{max} as a function of p.
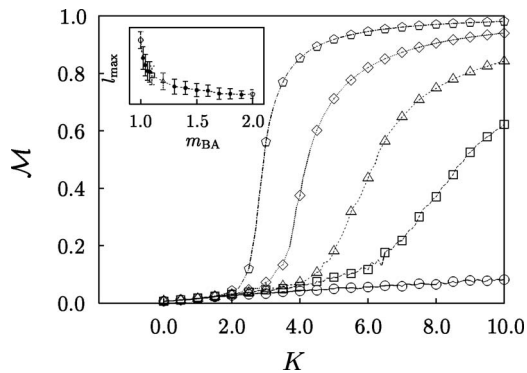
FIG. 6. The ST patterns as a function of K for various mean numbers of emanating edges of the BA model, $m_{BA}=1.0$ ($\bigcirc$), 1.1 ($\square$), 1.2 ($\triangle$), 1.4 ($\diamond$), and 2.0 ($\bigcirc$). Inset: Plot of ℓ_{max} as a function of m_{BA}.

increases, the edges connecting different branches are formed, and its fraction is non-negligible for $m_{BA} \geqslant 1.1$. As a result, the synchronization transition occurs more drastically for $m_{BA} \geqslant 1.1$. It was found that as m_{BA} increases, the exponent δ associated with the load distribution, $P_\ell(\ell) \sim \ell^{-\delta}$, increases drastically from $\delta \approx 2.0$, and almost remains as 2.2 for $m_{BA} \geqslant 1.1$ [21]. This fact is closely related to the crossover behavior of $\mathcal{M}$.

In summary, we have studied the two different types of the synchronization patterns on SF networks through a modified Kuramoto model. Such different patterns are mainly rooted from different types of intermodular connection profile. When the intermodular connections are decentralized (centralized), the ST occurs very drastically (gradually) and the synchronization arises globally (within modules), of which the behavior was analyzed quantitatively. We also showed that the ST point occurs at finite coupling constant for the former, while it is not well identified for the latter by performing finite-size scaling analysis. The critical exponent β associated with the order parameter is obtained to be $\beta \approx 1$ for the former case. The crossover behavior between the two cases was also studied by rewiring edges from the hierarchy model and by modifying the BA model. Finally, it is interesting to note that the global or the modular synchronization may be related to epileptic seizure. While the brain is electrically activated, any disruption within it may cause abnormal functioning. Then neurons in one hemisphere misfire and generate abnormal electrical activities, which spread to the other hemisphere through diverse pathways, leading to the global synchronization [22]. To treat it, the corpus callosum, the main communication pathways between the two hemispheres, is sometimes cut to prevent the communications from one side to the other. It is revealed through recent experiment [23] that while the synchronization after the cut arises within one module mostly, the global synchronization also arises occasionally, which is accomplished via other pathways.

[1] R. Albert and A.-L. Barabási, Rev. Mod. Phys. **74**, 47 (2002); S. N. Dorogovtsev and J. F. F. Mendes, Adv. Phys. **51**, 1079 (2002); M. E. J. Newman, SIAM Rev. **45**, 167 (2003).

[2] A.-L. Barabási and R. Albert, Science **286**, 509 (1999).

[3] E. Ravasz, A. L. Somera, D. A. Mongru, Z. N. Oltvai, and A.-L. Barabási, Science **297**, 1551 (2002).

[4] A. Rives and T. Galitski, Proc. Natl. Acad. Sci. U.S.A. **100**, 1128 (2003).

[5] K. A. Eriksen, I. Simonsen, S. Maslov, and K. Sneppen, Phys. Rev. Lett. **90**, 148701 (2003).

[6] M. Girvan and M. E. J. Newman, Proc. Natl. Acad. Sci. U.S.A. **99**, 8271 (2002).

[7] M. E. J. Newman and M. Girvan, Phys. Rev. E **69**, 026113 (2004).

[8] S. Jalan and R. E. Amritkar, Phys. Rev. Lett. **90**, 014101 (2003).

[9] S. H. Strogatz, Nature (London) **410**, 268 (2001), and references therein.

[10] J. T. Ariaratnam and S. H. Strogatz, Phys. Rev. Lett. **86**, 4278 (2001).

[11] For a list of references, for example, see A. T. Winfree, *The Geometry of Biological Time* (Springer-Verlag, New York, 1980); A. Pikovsky, M. Rosenblum, and J. Kurths, *Synchronization: A Universal Concept in Nonlinear Science* (Cambridge University Press, Cambridge, England, 2001).

[12] Y. Kuramoto, *Chemical Oscillations, Waves, and Turbulence* (Springer-Verlag, Berlin, 1984).

[13] A. E. Motter, C. Zhou, and J. Kurths, Europhys. Lett. **69**, 334 (2005).

[14] E. Oh, D. S. Lee, B. Kahng, and D. Kim (unpublished).

[15] T. Ichinomiya, Phys. Rev. E **70**, 026116 (2004).

[16] G. P. McCable, and D. S. Moore, *Introduction to the Practice of Statistics* (Freeman and Company, New York, 1996).

[17] E. Ravasz and A.-L. Barabási, Phys. Rev. E **67**, 026112 (2003).

[18] T. Nishikawa, A. E. Motter, Y.-C. Lai, and F. C. Hoppensteadt, Phys. Rev. Lett. **91**, 014101 (2003).

[19] H. Hong, B. J. Kim, M. Y. Choi, and H. Park, Phys. Rev. E **69**, 067105 (2004).

[20] K-I. Goh, B. Kahng, and D. Kim, Phys. Rev. Lett. **87**, 278701 (2001).

[21] C. M. Ghim *et al.*, Eur. Phys. J. B **38**, 305 (2004); K-I. Goh *et al.*, Phys. Rev. Lett. **91**, 189804 (2003).

[22] P. Conlon and M. R. Trimble, Epilepsy Res. **2**, 122 (1988).

[23] M. Vergnes *et al.*, Epilepsy Res. **4**, 8 (1989).